

Finite wavelength cloaking by plasmonic resonance

N-A P Nicorovici¹, R C McPhedran¹, S Enoch² and G Tayeb²

¹ CUDOS, School of Physics, University of Sydney, NSW 2006, Australia

² Institut Fresnel, CNRS, Aix-Marseille Université, 13013 Marseille, France

Abstract. We consider cloaking by a coated cylindrical system using plasmonic resonance, and extend previous quasistatic treatments to include the effect of finite wavelength. We show that a probe cylinder can still be cloaked at finite wavelengths, but the cloaking cylinder develops a non-zero scattering cross-section. We show that this latter effect is dominated by a monopole term in the case of an ideal (lossless) cloaking material, and by a dipole term in the case of a realistic (lossy) material. It can be reduced but not eliminated by variations of geometric or dielectric parameters of the cloaking cylinder.

PACS numbers: 78.20.-e, 41.20.-q, 42.25.Bs

Submitted to: *New J. Phys.*

1. Introduction

There is much current interest in the possibility of cloaking or hiding objects from scrutiny by electromagnetic waves. At least three techniques have been proposed to achieve this: one avoids detection by surrounding the target body with a metamaterial shell which guides light around the central cavity [1, 2], the second again relies on a metamaterial [3, 4, 5, 6, 7, 8], which this time cloaks by resonance an external region, while the third uses a structured metamaterial which provides cloaking by in effect folding space back upon itself [9, 10]. The technical challenges of making such systems in practice are enormous, but it should be realized that these and other proposals for cloaking offer complementary characteristics, which implies that work on a range of them is valuable.

Table 1. Comparison of three cloaking methods.

Mechanism	Refraction	Reaction	Unfolding
Region	Internal	External	External
Structure	Metamaterial Shell: $\epsilon, \mu \geq 0$ vary with position	Metamaterial homogeneous $\epsilon_s + \epsilon_m = 0$	Metamaterial Shell: $\epsilon, \mu \geq 0$ vary with position
Equations	2D, 3D Maxwell	2D quasistatics	2D, 3D quasistatics
Experiment	Yes	No	No
Problems	Bandwidth, structuring shell, energy dissipation.	Bandwidth, achieving ϵ_s , scale size $\ll \lambda$.	Bandwidth, structuring shell, scale size $\ll \lambda$.

We present a number of salient characteristics of the three methods in Table 1. Cloaking by refraction requires a structured metamaterial shell to divert light around a cavity in which the object to be hidden is placed (internal cloaking). It is designed using a full solution of Maxwell equations in two or three dimensions, and there has been an experimental demonstration of this mechanism in the former case [11]. The second and third methods offer the complementary feature of concealing a body in a region close to, but outside, the cloaking system (external cloaking). In the case of cloaking by reaction, the object is concealed by virtue of a plasmonic resonance, which requires the material in the cylindrical cloaking shell to have a dielectric constant close to the

negative of the dielectric constants in the core and matrix regions surrounding it. It has been studied to this point mainly in two dimensions. The third method is the most recent, and has features in common with each of the other two. It achieves cloaking by using a spatially varying dielectric constant and magnetic permeability, designed using the same principles of transformation optics at a basis of refractive cloaking. The goal here, however, is to in effect fold space back upon itself, and, loosely speaking, to hide the object within the enfolding.

It is our purpose here to study one problematic aspect of cloaking by reaction, which is implicit in two previous papers [7, 12], but which has not been studied systematically. The problem does not arise for cloaking by refraction or unfolding, by virtue of their different mechanism of operation, which ensures that both the cloaking system and the cloaked object are hidden to an equal degree from electromagnetic probes. As we shall see, this is not necessarily for cloaking by reaction, where it is quite possible for a larger cloaking system to successfully cloak a small object, but to be itself quite visible. Using a visual analogy from the animal kingdom, we refer to this as "Ostrich Effect": *the large object hides the small object, but the large object does not hide itself*. The possibility of the Ostrich Effect, was signaled in a paper by Milton, Brian and Willis [13]: "Besides invisibility there is what we call cloaking where the surrounding material does not have to be carefully adapted to suit the object to be made invisible. The cloaking device may be invisible or visible, although obviously the former is more interesting."

We take the viewpoint here that for many purposes, the Ostrich Effect will be undesirable, and so we provide examples of the effect, explore its underlying physics, and quantify the circumstances under which it is greatly reduced. In Sec. II we present two figures taken from simulations showing the quenching of the dipole moment of a probe cylinder in the vicinity of a cylindrical shell with realistic values of the complex dielectric constant. These figures illustrate clearly the Ostrich Effect. In the next Section we consider a coated cylinder interacting with an incident plane wave and solve this scattering problem in closed form. We also take the long wavelengths limit of the formulation, in order to exhibit the transition from dynamics to qualitative. In Sec. IV we use the scattering cross section of the coated cylinder to show the counterintuitive result that a small imaginary part of ε_s actually benefits cloaking at finite wavelengths, since it makes dipole rather than monopole terms dominant in the scattering cross section. This is in keeping with the results of Hao-Yuan She *et al* [14] but not with those reported by Min Yan *et al* [15].

2. Description of cloaking numerical simulations

Let us consider a two-dimensional physical system comprising a coated cylinder centred about the origin of coordinates and a probe (solid) cylinder on the y-axis. Both cylinders are perpendicular to the xy -plane. The shell and core radii of the coated cylinder are, respectively, $r_c = 20\text{nm}$, $r_s = 65\text{nm}$, while the radius of the probe cylinder is $a = 5\text{nm}$. Also, the core and shell relative permittivities are $\varepsilon_c = 1$, $\varepsilon_s = -1 + 0.1i$. The relative

permittivity of the probe cylinder is $\varepsilon = \varepsilon_s$ and the relative permittivity of the matrix is $\varepsilon_m = 1$. All the components are non-magnetic so that the relative permeabilities are $\mu_c = \mu_s = \mu = \mu_m = 1$, where μ is the permeability of the probe cylinder.

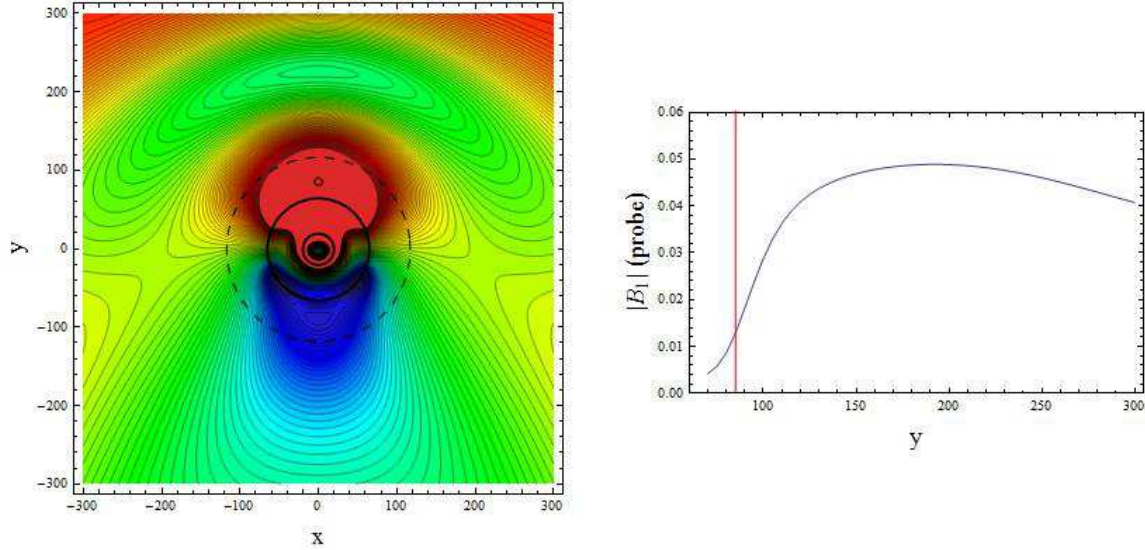


Figure 1. Left: Contour plot of $|H_z|$ as a function of position for a system consisting of a coated cylinder ($r_c = 20\text{nm}$, $r_s = 65\text{nm}$, $\varepsilon_c = 1$, $\varepsilon_s = -1 + 0.1i$, $\mu_c = \mu_s = 1$) interacting with a probe cylinder ($a = 5\text{nm}$, $\varepsilon = -1 + 0.1i$, $\mu = 1$), and irradiated by a H_z polarized plane wave with wavelength 600nm coming from above. The probe cylinder is within the cloaking region bounded by the dashed circle, at a distance of 85nm from the origin. Right: magnitude of the dipole moment of the probe cylinder as a function of its position indicated by the red line. The magnetic field varies in the range $0.63 \leq |H_z| \leq 1.79$, whereas the incident plane wave is normalized to $|H_z^{(inc)}| = 1$

This physical system is subjected to an incident plane wave having $\lambda = 600\text{nm}$ and with the wave vector in the xy -plane (in-plane incidence) and polarized with the magnetic field parallel to the cylinder axes (H_z polarization).

The probe cylinder is polarisable, and has a dipole moment proportional to the total electric field at its position. When the probe cylinder moves along the y -axis and enters the cloaking region, marked by the dashed circle in figures 1 and 2, one can see the effect of cloaking, in the sense that the dipole moment of the probe cylinder tends to zero within the cloaking circle of radius $r_{\#} = \sqrt{(r_s^3/r_c)}$ [6, 7] (see figure 1, right panel). Consequently, the probe cylinder is successfully cloaked within $r_{\#}$ but not of course outside it, compare the left panels of figures 1 and 2. Nevertheless, the cloaking system is not invisible, since the coated cylinder distorts the incident plane wave. Note that figures 1 and 2 are frames in the animation available with this paper, which illustrates the quenching of the dipole moment of the probe cylinder within the cloaking circle, and its re-emergence outside it.

The relative permittivity value chosen for the shell in figures 1 and 2 is comparable to that of silicon carbide near $\lambda = 10\mu\text{m}$ [16], and has an imaginary part somewhat lower than that of silver at the wavelength in the ultraviolet where the real part of its

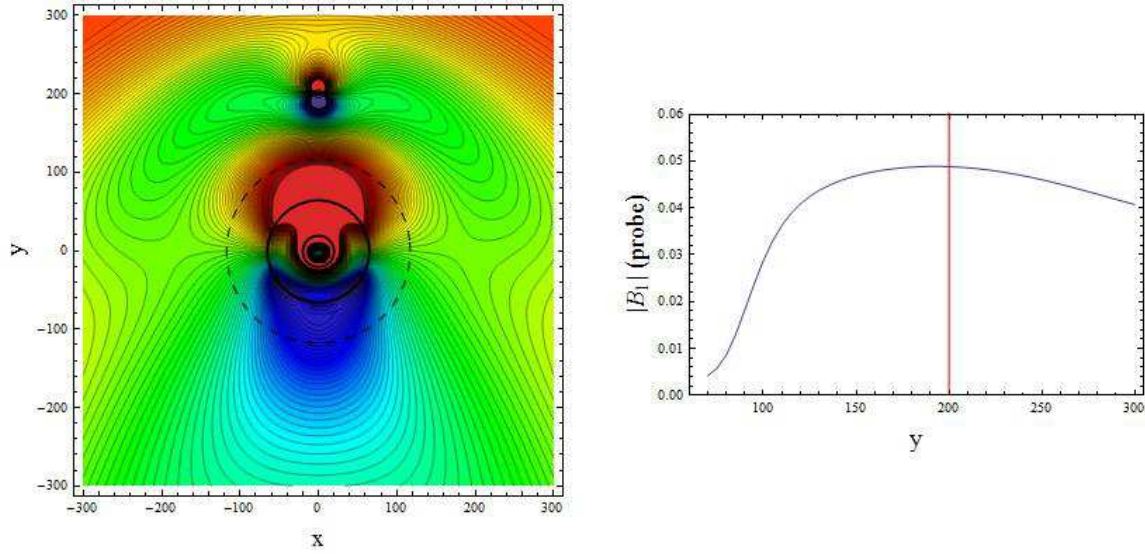


Figure 2. As for Fig. 1 with the probe cylinder outside the cloaking region. Now, the probe is at a distance of 200nm from the origin, and $0.21 \leq |H_z| \leq 1.81$.

permittivity passes through -1. While we refer to distances in nanometers, in practice the relevant parameter is the wavelength of the incident radiation divided by a characteristic length, say the outer radius r_s of the coated cylinder. Hence, the results shown in figures 1 and 2 and subsequent figures can be easily applied to systems rescaled to correspond to materials other than those mentioned.

Note that in the previous figures and simulations we have presented [6, 7, 8] to illustrate resonant cloaking, the value of the imaginary part of ϵ_s was chosen to correspond to the mathematical analysis, rather than to practical materials. We have found that good quenching of the dipole moment of the probe particle can be achieved even with quite significant imaginary parts for ϵ_s , provided $r_{\#}$ is sufficiently in excess of r_s , so that the probe particle can move deep within the cloaking region.

Despite the quite effective cloaking of the probe cylinder shown in the right panels of figures 1 and 2, the left panels illustrate strong distortion of the incident wave in the vicinity of the cloaking cylinder. Such variations of magnetic field strength would compromise any attempts to hide the compound system of cloaking cylinder plus probe.

We mention that in all numerical computations we have used the scattering-matrix method [17], which is based on the expansion of the fields in terms of Fourier-Bessel series around each cylinder. By using the scattering matrices of each cylinder and the translation properties of Fourier-Bessel functions, the method leads to the inversion of a linear set of equations.

3. The quasistatic limit

For a coated cylinder centered at the origin of coordinates, we represent the electric and magnetic fields E_z and H_z (denoted here by V), by series expansions in terms of

cylindrical harmonics [18]:

$$V(r, \theta, z, t) = \sum_{\ell=-\infty}^{\infty} \left\{ \begin{array}{l} A_{\ell}^c J_{\ell}(k_c r) e^{i\ell\theta} \\ \left[A_{\ell}^s J_{\ell}(k_s r) + B_{\ell}^s H_{\ell}^{(1)}(k_s r) \right] e^{i\ell\theta} \\ \left[A_{\ell}^m J_{\ell}(k_m r) + B_{\ell}^m H_{\ell}^{(1)}(k_m r) \right] e^{i\ell\theta} \end{array} \right\} e^{i(\beta z - \omega t)}, \quad (1)$$

where $J_{\ell}(\cdot)$ and $H_{\ell}^{(1)}(\cdot)$ represent the Bessel and Hankel functions of the first kind. The three forms of the series expansions in (1) correspond to the domains $0 \leq r \leq r_c$ (inside the core of the coated cylinder), $r_c \leq r \leq r_s$ (inside the shell of the coated cylinder) and $r \geq r_s$ (in the matrix), respectively. Also, the superscripts c , s and m label the fields inside the cylinder core, cylinder shell, and in the matrix, respectively. Thus, we have the wavenumbers $k_c^2 = \omega^2 \varepsilon_c \mu_c$, $k_s^2 = \omega^2 \varepsilon_s \mu_s$, and $k_m^2 = \omega^2 \varepsilon_m \mu_m$.

The function V has to satisfy the boundary conditions, i.e., the continuity of the tangential components of the electric (E_z and E_{θ}) and magnetic (H_z and H_{θ}) fields across the core and shell surfaces. When the coated cylinder is subjected to an incident radiation which is perpendicular to the axis of the cylinder, we have $\beta = 0$, and the problem can be reduced to solving two independent problems [19]:

- E_z polarization, when $H_z = 0$ and the transverse parts of \mathbf{H} are generated by ∇E_z , and
- H_z polarization, when $E_z = 0$ and ∇H_z gives the transverse components of \mathbf{E} .

In the present analysis we are interested in the relation between the coefficients in the matrix, which has the form

$$A_{\ell}^m = -M_{\ell} B_{\ell}^m. \quad (2)$$

The coefficients A_{ℓ}^m are determined by the sources of the field applied to the structure, and satisfy the field identity [8]

$$\sum_{\ell=-\infty}^{\infty} A_{\ell}^m J_{\ell}(k_m r) e^{i\ell\theta} = \text{source field}. \quad (3)$$

Hence, we obtain the coefficients A_{ℓ}^m by expanding the source field in terms of cylindrical harmonics $J_{\ell}(k_m r) e^{i\ell\theta}$.

Here, we also consider that the field applied to the physical structure is a plane wave field. In cylindrical coordinates, for H_z polarization ($H_x = H_y = 0$), a magnetic plane wave is described by the formula

$$H_z^{\text{PW}}(r, \varphi, z) = H_0 e^{i[k_0 r \cos(\varphi - \psi_0) + k_z z]}, \quad (4)$$

where ψ_0 is the angle of incidence with respect to the x-axis. We consider the case of in-plane incidence ($k_z \equiv \beta = 0$) so that the exponential in (4) can be expanded in terms of Bessel functions of the first kind

$$H_z^{\text{PW}}(r, \varphi) = H_0 \sum_{n=-\infty}^{\infty} i^n J_n(k_0 r) e^{in(\varphi - \psi_0)}. \quad (5)$$

Consequently, for a coated cylinder subjected to a plane wave incoming field, perpendicular to the cylinder axis, we have the coefficients

$$A_n^m = H_0 i^n e^{-in\psi_0}, \quad (6)$$

where

$$\psi_0 = \begin{cases} \pi, & \text{if the radiation comes from } x = +\infty, \\ 0, & \text{if the radiation comes from } x = -\infty. \end{cases} \quad (7)$$

In the case of E_z polarization we obtain an equation identical to (6) for the coefficients of the electric field.

3.1. H_z Polarization

We concentrate now on a coated cylinder, centered about the origin of coordinates, made from non-magnetic materials for which $\mu_m = \mu_s = \mu_c = \mu_0$, so that $\varepsilon_m = n_m^2 \varepsilon_0$, $\varepsilon_s = n_s^2 \varepsilon_0$ and $\varepsilon_c = n_c^2 \varepsilon_0$, where ε_0 is the dielectric constant of free space, and n_i ($i = m, s, c$) represent the refractive indexes of the matrix, shell and core, respectively. The boundary conditions coefficients M_ℓ from (2), are derived by eliminating A_ℓ^c in the equations [18]

$$\begin{aligned} \begin{bmatrix} A_\ell^m \\ B_\ell^m \end{bmatrix} &= \begin{bmatrix} J_\ell(k_m r_s) & H_\ell(k_m r_s) \\ Z_m J'_\ell(k_m r_s) & Z_m H'_\ell(k_m r_s) \end{bmatrix}^{-1} \begin{bmatrix} J_\ell(k_s r_s) & H_\ell(k_s r_s) \\ Z_s J'_\ell(k_s r_s) & Z_s H'_\ell(k_s r_s) \end{bmatrix} \\ &\times \begin{bmatrix} J_\ell(k_s r_c) & H_\ell(k_s r_c) \\ Z_s J'_\ell(k_s r_c) & Z_s H'_\ell(k_s r_c) \end{bmatrix}^{-1} \begin{bmatrix} J_\ell(k_c r_c) & H_\ell(k_c r_c) \\ Z_c J'_\ell(k_c r_c) & Z_c H'_\ell(k_c r_c) \end{bmatrix} \begin{bmatrix} A_\ell^c \\ 0 \end{bmatrix}, \end{aligned} \quad (8)$$

where $J_\ell(\cdot)$ and $H_\ell(\cdot) \equiv H_\ell^{(1)}(\cdot)$ are Bessel and Hankel functions of the first kind, the prime indicates the derivative of the corresponding function, and $Z_i = \sqrt{\mu_i/\varepsilon_i}$ ($i = m, s, c$) represent the impedances of the matrix, shell and core, respectively. For E_z polarization we obtain the relation between A_ℓ^m and B_ℓ^m by changing $Z_i \rightarrow 1/Z_i$ in (8).

In the quasistatic limit ($k_m \rightarrow 0$), we approximate the Bessel functions by the first term in their series expansion, i.e.

$$J_0(z) \approx 1 - \left(\frac{z}{2}\right)^2,$$

$$J_n(z) \approx \begin{cases} \frac{1}{n!} \left(\frac{z}{2}\right)^n & \text{for } n \geq 0, \\ (-1)^n \frac{1}{(-n)!} \left(\frac{z}{2}\right)^{-n} & \text{for } n < 0, \end{cases}$$

$$H_0(z) \approx J_0(z) + i \frac{2}{\pi} \left[\gamma^E + \log\left(\frac{z}{2}\right) \right],$$

$$H_n(z) \approx J_n(z) + i \begin{cases} -\frac{1}{\pi} \left(\frac{2}{z}\right)^n (n-1)! & \text{for } n \geq 0, \\ (-1)^{n+1} \frac{1}{\pi} \left(\frac{2}{z}\right)^{-n} (-n-1)! & \text{for } n < 0, \end{cases}$$

where γ^E is the Euler-Mascheroni constant [20]. Then, we substitute these expressions in (8) and write M_ℓ as a fraction. Using the limit $k_m \rightarrow 0$ we determine the coefficient of k_m^0 in the numerator and the coefficient of $k_m^{2\ell}$ in the denominator. Thus, the quasistatic limit of M_ℓ for $\ell \geq 0$ is

$$M_\ell = M_{-\ell} \approx -\frac{i}{\pi} \left(\frac{2}{k_m r_s}\right)^{2\ell} \ell! (\ell-1)! \gamma_\ell, \quad (9)$$

where

$$\gamma_\ell = \frac{r_c^{2\ell}(\varepsilon_s - \varepsilon_c)(\varepsilon_m - \varepsilon_s) + r_s^{2\ell}(\varepsilon_s + \varepsilon_c)(\varepsilon_m + \varepsilon_s)}{r_c^{2\ell}(\varepsilon_s - \varepsilon_c)(\varepsilon_m + \varepsilon_s) + r_s^{2\ell}(\varepsilon_s + \varepsilon_c)(\varepsilon_m - \varepsilon_s)}. \quad (10)$$

For $\ell = 0$, we obtain a completely different form

$$M_0 \approx -\frac{i}{\pi} \left(\frac{2}{k_m r_s}\right)^4 \frac{\varepsilon_m}{(\varepsilon_s - \varepsilon_c)(r_c/r_s)^4 + (\varepsilon_m - \varepsilon_s)}. \quad (11)$$

Note that in all these calculations we made no assumption about the nature (real or complex) of permittivities or refractive indices.

To relate the long wavelength limit of the dynamic problem with the corresponding problem in electrostatics we apply the same method as in Ref. [21]. Thus, the boundary conditions for our problem correspond to an electrostatic problem in which the inverse of the dielectric constants ($\varepsilon_c \rightarrow 1/\varepsilon_c$, $\varepsilon_s \rightarrow 1/\varepsilon_s$ and $\varepsilon_m \rightarrow 1/\varepsilon_m$) have to be considered. This will also change $\gamma_\ell \rightarrow -\gamma_\ell$. Now, the boundary conditions (2) for $\ell \neq 0$ can be written in the form

$$A_\ell^m \approx -\frac{i}{\pi} \left(\frac{2}{k_m}\right)^{2\ell} \ell! (\ell-1)! \gamma_\ell \frac{B_\ell^m}{r_s^{2\ell}}. \quad (12)$$

Note that, here, we separated the product $k_m r_s$, which is dimensionless, so that k_m and r_s are considered as multiplied, respectively divided, by a length unit.

In electrostatics, the corresponding relationship between the coefficients A_ℓ and B_ℓ which controls the response of a coated cylinder to an external field, has the form [3, 4]

$$\tilde{A}_\ell = \gamma_\ell \frac{\tilde{B}_\ell}{r_s^{2\ell}}. \quad (13)$$

Now, by comparing (12) with (13) we may infer the relation between static and dynamic multipole coefficients

$$\tilde{B}_\ell \approx -\frac{i}{\pi} \left(\frac{2}{k_m}\right)^{2\ell} \ell! (\ell-1)! B_\ell^m \approx \frac{H_\ell(k_m)}{J_\ell(k_m)} B_\ell^m, \quad \text{for } \ell \neq 0. \quad (14)$$

Note that k_m is dimensionless according to the note after (12).

In electrostatics, the partial resonances of a three-phase composite consisting of coated cylinders are defined by the equations [3, 4]

$$\varepsilon_c + \varepsilon_s = 0 \quad (\text{core - shell resonance}), \quad (15)$$

$$\varepsilon_s + \varepsilon_m = 0 \quad (\text{shell - matrix resonance}), \quad (16)$$

when (13) becomes

$$\tilde{A}_\ell = \frac{\varepsilon_m + \varepsilon_c}{\varepsilon_m - \varepsilon_c} \frac{\tilde{B}_\ell}{r_s^{2\ell}}, \quad (17)$$

or

$$\tilde{A}_\ell = \frac{\varepsilon_m + \varepsilon_c}{\varepsilon_m - \varepsilon_c} \frac{\tilde{B}_\ell}{(r_s^2/r_c)^{2\ell}}, \quad (18)$$

respectively. In the first case, the field inside the coated cylinder is exactly the same as would be found within a solid cylinder of radius r_s and dielectric constant ε_c , while the potential outside the coated cylinder, in the matrix, is precisely the same as that outside the solid cylinder [6, 3]. The second case corresponds to a solid cylinder of radius $r_s^2/r_c > r_s$ (the geometrical image of the core boundary with respect to the shell outer boundary), and dielectric constant ε_c . Now, the field external to the coated cylinder *and beyond the radius* $r_* = r_s^2/r_c$ is the same as that external to the solid cylinder [6, 3].

Since it is the relationship between the coefficients A_ℓ^m and B_ℓ^m which controls the response of a coated cylinder to an external field, equations (13) and (12) show that this response is determined by γ_ℓ in electrostatics as well as in the long wavelengths limit of electrodynamics. The limiting process is smooth and therefore, we expect a resonant behavior accompanied by cloaking effects, even for nonzero frequencies, when one of the conditions (15) or (16) is satisfied.

3.2. E_z Polarization

Now, in the long wavelength limit, the boundary conditions coefficients M_ℓ from (2) take the form

$$M_\ell = M_{-\ell} \approx -\frac{i}{\pi} \left(\frac{2}{k_m r_s} \right)^{2\ell+2} \frac{2\ell!(\ell+1)!\varepsilon_m}{(\varepsilon_s - \varepsilon_c)(r_c/r_s)^{2\ell+2} + (\varepsilon_m - \varepsilon_s)}, \quad (19)$$

for $\ell \neq 0$, and

$$M_0 \approx -\frac{i}{\pi} \left(\frac{2}{k_m r_s} \right)^2 \frac{\varepsilon_m}{(\varepsilon_s - \varepsilon_c)(r_c/r_s)^2 + (\varepsilon_m - \varepsilon_s)}. \quad (20)$$

Note that there are no terms of the form $\varepsilon_c + \varepsilon_s$ or $\varepsilon_s + \varepsilon_m$ in (19) or (20) to indicate a core-shell or shell-matrix partial resonance. Again, the limiting process is smooth and, consequently, we do not expect a resonant behaviour of the coated cylinder, for any frequency, in the case of E_z polarization. Consequently, when the coated cylinder is irradiated with a field of a general polarization, that is a mixture of H_z and E_z polarizations, or in the case of conical incidence, the cloaking by resonance will never be perfect, or even may be completely ruined, due to the contribution of the E_z polarized component.

Resonances similar to those in Sec. 8 can occur in the case of a coated cylinder made from magnetic metamaterials with permittivity ε_0 and permeabilities μ_c , μ_s , and μ_m . Now, the boundary conditions coefficients M_ℓ from (2) take the forms (9) and (11) with ε_i replaced by μ_i [18, 14]. Hence, the magnetic partial resonances of coated cylinders are defined by the equations

$$\mu_c + \mu_s = 0 \quad (\text{core} - \text{shell resonance}), \quad (21)$$

$$\mu_s + \mu_m = 0 \quad (\text{shell} - \text{matrix resonance}). \quad (22)$$

4. Attempts to minimize the Ostrich Effect

As a measure of effectiveness of cloaking we choose the total scattering cross section. For two-dimensional problems, the total scattering cross section is defined as the ratio of the total power scattered by an object, to the incident power per unit length [19, 22]

$$\sigma_t = \frac{4}{k_m} \sum_{\ell=-\infty}^{\infty} |B_\ell^m|^2 = \frac{4}{k_m} |B_0^m|^2 + \frac{8}{k_m} \sum_{\ell=1}^{\infty} |B_\ell^m|^2. \quad (23)$$

Here, the B_ℓ^m coefficients have the exact form given by (8), that is

$$B_\ell^m = \frac{P}{Q} A_\ell^m, \quad (24)$$

where

$$\begin{aligned} P = & \{ [Z_m J'_\ell(k_m r_s) J_\ell(k_s r_s) - Z_s J_\ell(k_m r_s) J'_\ell(k_s r_s)] \\ & \times [Z_c H_\ell(k_s r_c) J'_\ell(k_c r_c) - Z_s H'_\ell(k_s r_c) J_\ell(k_c r_c)] \} \\ & - \{ [Z_s H'_\ell(k_s r_s) J_\ell(k_m r_s) - Z_m H_\ell(k_s r_s) J'_\ell(k_m r_s)] \\ & \times [Z_s J'_\ell(k_s r_c) J_\ell(k_c r_c) - Z_c J_\ell(k_s r_c) J'_\ell(k_c r_c)] \}, \end{aligned}$$

$$\begin{aligned} Q = & \{ [Z_m H'_\ell(k_m r_s) J_\ell(k_s r_s) - Z_s H_\ell(k_m r_s) J'_\ell(k_s r_s)] \\ & \times [Z_s H'_\ell(k_s r_c) J_\ell(k_c r_c) - Z_c H_\ell(k_s r_c) J'_\ell(k_c r_c)] \} \\ & - \{ [Z_m H'_\ell(k_m r_s) H_\ell(k_s r_s) - Z_s H_\ell(k_m r_s) H'_\ell(k_s r_s)] \\ & \times [Z_s J'_\ell(k_s r_c) J_\ell(k_c r_c) - Z_c J_\ell(k_s r_c) J'_\ell(k_c r_c)] \}, \end{aligned}$$

and with A_ℓ^m from (6) for $E_0 = 1$ and $\psi = 0$.

In the case of the resonance $\varepsilon_c = \varepsilon_m = 1$ and $\varepsilon_s = -1$, numerical simulations show that by using the form (24) and the series (23) truncated to $N_{\text{trunc}} = 6$, we have

$$\sigma_t^{(N_{\text{trunc}})} = \frac{4}{k_m} \sum_{\ell=-N_{\text{trunc}}}^{N_{\text{trunc}}} |B_\ell^m|^2 \approx \frac{4}{k_m} |B_0^m|^2 = \sigma_t^{(0)}, \quad (25)$$

starting at about $\lambda = 10 r_s$ (see figure 3). From the same wavelength up, the contribution of the dipole terms, given by $\sigma_t^{(1)} - \sigma_t^{(0)}$, becomes very small.

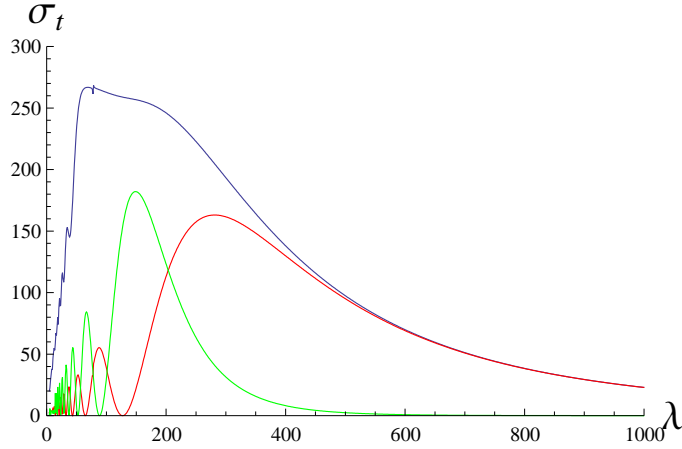


Figure 3. Total cross section $\sigma_t^{(6)}$ (blue curve), $\sigma_t^{(0)}$ (red curve) from (25), and $\sigma_t^{(1)} - \sigma_t^{(0)}$ (green curve) as functions of the wavelength of the incident plane wave, for a coated cylinder ($r_c = 20\text{nm}$, $r_s = 65\text{nm}$) at resonance ($\varepsilon_c = \varepsilon_m = 1$, $\varepsilon_s = -1$, $\mu_c = \mu_s = \mu_m = 1$).

If we use the expression of B_ℓ^m in the quasistatic limit (see Sec. 3.1), with A_ℓ^m from (6), $E_0 = 1$, and $\psi = 0$, we obtain

$$B_\ell^m \approx \begin{cases} i \pi^5 \frac{(\varepsilon_s - \varepsilon_c)(r_c/r_s)^4 + (\varepsilon_m - \varepsilon_s)}{\varepsilon_m} \left(\frac{r_s}{\lambda}\right)^4, & \text{for } \ell = 0, \\ i^{l+1} \pi^{2l+1} \frac{1}{\ell! (\ell-1)! \gamma_\ell} \left(\frac{r_s}{\lambda}\right)^{2\ell}, & \text{for } \ell \geq 1. \end{cases} \quad (26)$$

In the case of core-shell-matrix resonance, that is $\varepsilon_c + \varepsilon_s = 0$ and $\varepsilon_s + \varepsilon_m = 0$, the coefficient γ_ℓ defined in (10) tends to infinity so that, for $\ell \geq 1$, $B_\ell^m \rightarrow 0$. Such a situation arises when

$$\varepsilon_c = -\varepsilon_s = \varepsilon_m \quad (27)$$

(as in the case of $\varepsilon_c = \varepsilon_m = 1$ and $\varepsilon_s = -1$), and the total scattering cross section is determined only by the zeroth-order multipole

$$\sigma_t^{\text{QS}} \approx \frac{4}{k_m} |B_0^m|^2 \propto \left(\frac{r_s}{\lambda}\right)^7, \quad (28)$$

which tends rapidly to zero as the wavelength increases. Actually, B_0^m from (24) tends very slowly to the form (26). This last form has been obtained by taking the first term in the series of all Bessel functions, except $J_0(z)$ and $H_0(z)$). For complicated expressions like (24) the series expansions require more terms for accuracy, as they contain products of four Bessel functions.

The main result is that for long wavelengths σ_t is determined by the B_0^m , only. The dominance of zeroth-order multipole is also present in the case of coordinate transformation method [1]. This case has been analyzed by Yan *et al* [15].

Here, we have considered that $\varepsilon_s = -1$ is real, which is unphysical. Physical materials with negative permittivity (usually metals) are lossy so that we have to

consider a coated cylinder with the shell material having a complex permittivity $\varepsilon_s = -1 + i\delta$, where $\delta > 0$ determines the loss in the shell. A detailed analysis of this case shows that, in the limit of long wavelengths, the total cross section σ_t is now dominated by the dipole coefficients $B_{\pm 1}^m$.

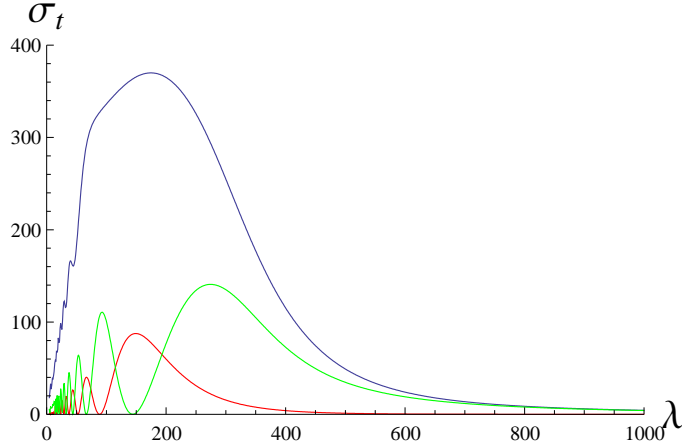


Figure 4. Total cross section $\sigma_t^{(6)}$ (blue curve), $\sigma_t^{(0)}$ (red curve) from (25), and $\sigma_t^{(1)} - \sigma_t^{(0)}$ (green curve) as functions of the wavelength of the incident plane wave, for a coated cylinder ($r_c = 20\text{nm}$, $r_s = 65\text{nm}$) at resonance ($\varepsilon_c = \varepsilon_m = 1$, $\varepsilon_s = -1 + 0.1i$, $\mu_c = \mu_s = \mu_m = 1$).

We start with the analytic form of B_ℓ^m coefficients (24) and set the factor $A_\ell^m = 1$. In fact, A_ℓ^m defined in (6) has the modulus $|A_\ell^m| = E_0^2$ and we consider $E_0 = 1$. Now, for a finite δ , from the exact form (24) we obtain the following series expansion

$$B_0^m = a_4(\delta) k_0^4 + a_6(\delta) k_0^6 + \mathcal{O}(k_0^8), \quad (29)$$

where

$$a_4(\delta) = i\frac{\pi}{16}(r_c^4 - r_s^4) + \frac{\pi}{32}(r_c^4 - r_s^4)\delta, \quad (30)$$

$$a_6(\delta) = i\frac{\pi}{32}(r_c^6 - 2r_c^4 r_s^2 + r_s^6) + \frac{\pi}{192}(7r_c^6 - 12r_c^4 r_s^2 + 5r_s^6)\delta - i\frac{\pi}{192}(2r_c^6 - 3r_c^4 r_s^2 + r_s^6)\delta^2. \quad (31)$$

It is easy to check that the first term in the limit

$$\lim_{\delta \rightarrow 0} B_0^m = i\frac{\pi}{16}(r_c^4 - r_s^4) k_0^4 + i\frac{\pi}{32}(r_c^6 - 2r_c^4 r_s^2 + r_s^6) k_0^6 + \mathcal{O}(k_0^8), \quad (32)$$

is of the form (26) for $\ell = 0$, if we set $\varepsilon_c = \varepsilon_m = 1$ and $\varepsilon_s = -1$ in (26). Consequently, the behaviour of B_0^m as function of k_0 and δ , in the domain of long wavelengths, can be summarized as

$$B_0^m \simeq \begin{cases} a_4(\delta) k_0^4 & \text{if } \delta \neq 0, \\ a_4(0) k_0^4 & \text{if } \delta = 0. \end{cases} \quad (33)$$

Now, we analyze the dipole term B_1^m . Firstly, from (24) we obtain

$$B_1^m = b_2(\delta) k_0^2 + b_4(\delta) k_0^4 + \mathcal{O}(k_0^6), \quad (34)$$

where

$$b_2(\delta) = \frac{\pi r_s^2(r_s^2 - r_c^2)(2 - i\delta)}{4(-r_s^2\delta^2 + r_c^2(2 + i\delta))} \delta = \frac{\pi r_s^2(r_c^2 - r_s^2)}{8r_c^2} \delta + i \frac{\pi r_s^2}{16r_c^2} (r_c^2 - r_s^2)\delta^2 + \mathcal{O}(\delta^3), \quad (35)$$

$$b_4(\delta) = -i \frac{\pi}{8} r_s^4 \log\left(\frac{r_c}{r_s}\right) - \frac{\pi}{8} r_s^4 \log\left(\frac{r_c}{r_s}\right) \delta + \mathcal{O}(\delta^2). \quad (36)$$

We also have

$$\lim_{\delta \rightarrow 0} B_1^m \simeq -i \frac{\pi}{8} r_s^4 \log\left(\frac{r_c}{r_s}\right) k_0^4, \quad (37)$$

Finally, the behaviour of B_1^m as function of k_0 and δ , in the domain of long wavelengths, can be summarized as

$$B_1^m \simeq \begin{cases} b_2(\delta) k_0^2 & \text{if } \delta \neq 0, \\ b_4(0) k_0^4 & \text{if } \delta = 0. \end{cases} \quad (38)$$

It follows that, in the long wavelength limit, the scattering cross section is dominated by the monopole term $\sigma_t^{(0)} = 4|B_0^m|^2/k_m$ if $\delta = 0$, and by the dipole term $\sigma_t^{(1)} - \sigma_t^{(0)} = 8|B_1^m|^2/k_m$ when $\delta \neq 0$. This last result agrees with that obtained by Alu and Engheta [5] who have also shown that the dipole term dominates the scattering cross section, for lossy materials.

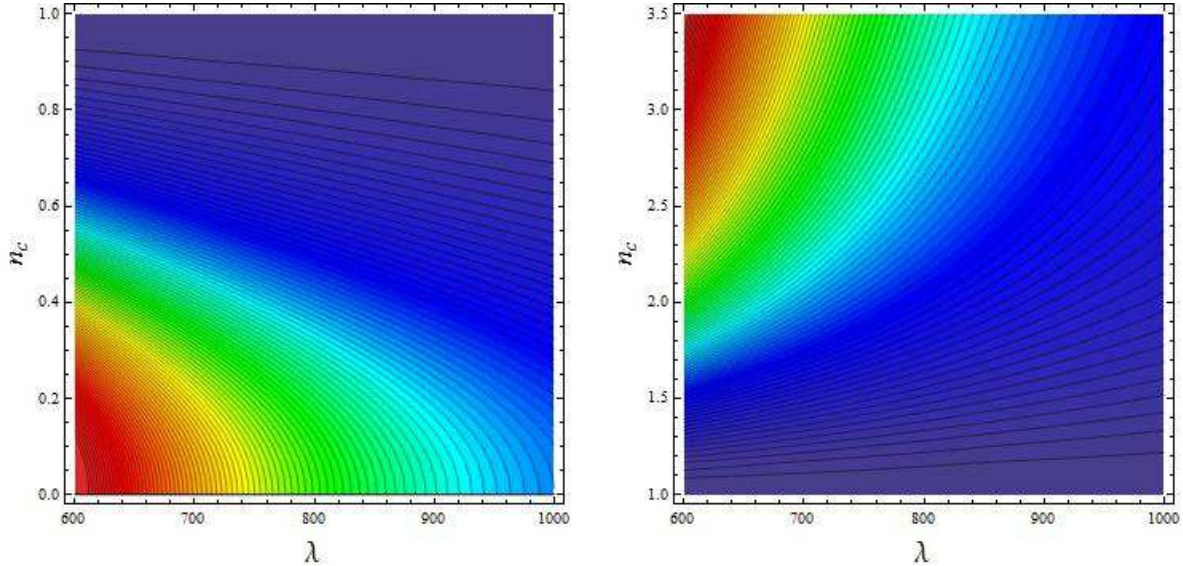


Figure 5. Scattering cross section $\sigma_t^{(6)}$, from equation (23), as a function of wavelength (λ) and core refractive index (n_c). Left: $n_c < 1$. Right: $n_c > 1$. The parameters of the physical system are: $r_c = 20\text{nm}$, $r_s = 65\text{nm}$, $\varepsilon_c = 1$, $\varepsilon_s = -1 + 0.1i$, $\mu_c = \mu_s = 1$. Red indicates large cross sections (up to 18.0), while blue indicates smaller values (down to 0.13).

Figure 4 shows the cross section σ_t as a function of wavelength calculated now for a realistic value $\varepsilon_s = -1 + 0.1i$ of the dielectric constant of the shell. In comparison with figure 3, we see that the dominant contribution to the cross section now comes from the

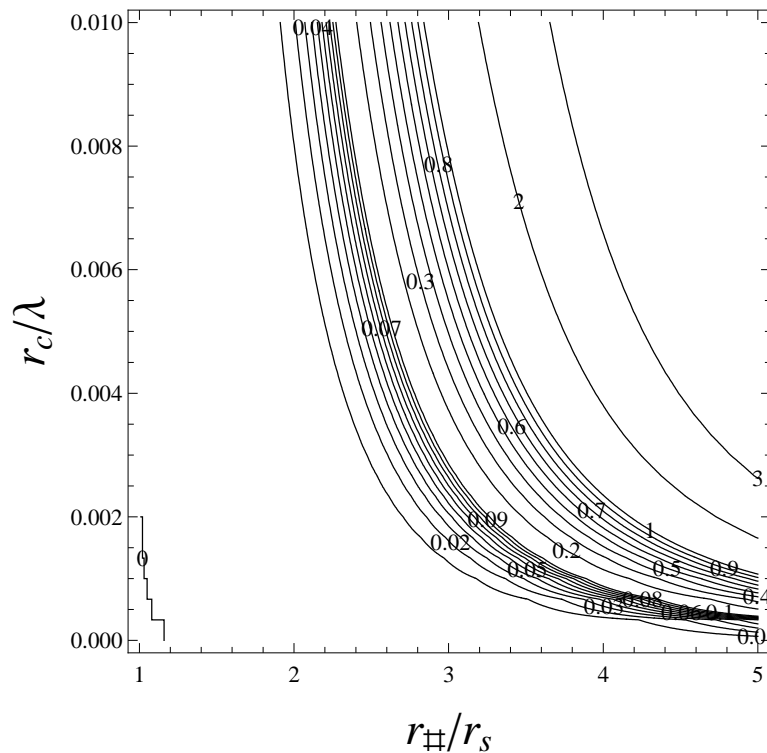


Figure 6. Normalized scattering cross section $\sigma_t^{(6)}/2r_s$, from equation (23), as a function of normalized core radius (r_c/λ) and $r_{\#}/r_s = \sqrt{r_s/r_c}$. Here $\varepsilon_c = 1$, $\varepsilon_s = -1 + 0.1i$, $\mu_c = \mu_s = 1$.

dipole terms rather than the monopole terms. Despite this difference, the cross section is well approximated by its leading term when the wavelength reaches around 10 times the shell radius. Note that in figure 3 the cross section varies as approximately $1/\lambda^2$ in the region of λ between 600 and 1000; this is far from the quasistatic behaviour of $1/\lambda^7$ expected from equation (33), showing that for this ideal case the cross section is not well represented by quasistatics even at $\lambda = 1000$. By contrast, for figure 4 the cross section goes as $1/\lambda^3$, in line with the quasistatic estimate (see equation (38), and also Panicky and Phillips [19]).

We can examine whether the Ostrich Effect can be reduced by making appropriate choices of the free parameters of the cloaking system: n_c , r_c and r_s . We study the effect on the scattering cross section of varying these parameters in figures 5 and 6. Figure 5 shows the effect of varying the core index, both below and above the value of unity used in previous figures. While the effect of n_c varies with wavelength, in general one sees from figure 5 that values around unity deliver the lowest cross sections. In figure 6 we study the effect on cross section of varying radii. Here, the cross section values have been normalized by dividing by the cylinder diameter, to give a dimensionless value. The geometric parameters r_c is shown divided by the wavelength, while the horizontal axis gives the cloaking radius $r_{\#}$ divided by r_s . The leftmost curve gives the contour on which the cross section is equal to 1% of the geometric value. Along this contour,

if we want to have say $r_{\#} = 2.5r_s$, to give a relatively large cloaked region, we need $r_c \simeq 0.003\lambda$ and $r_s \simeq 6.25r_c$, or $r_s \simeq 0.019\lambda$. These relatively strict tolerances illustrate the difficulty of achieving low cross section values at finite wavelengths. Figures 7 (a) and (b), show two field distributions corresponding to the probe inside and outside the cloaking region, with $\text{Im}(\varepsilon_s)$ now set to 0.01, in order to make more effective the cloaking action. We can see in these figures that we have achieved a satisfactory combination of effective cloaking of the probe and virtual elimination of the Ostrich Effect. We can quantify this by introducing a dimensionless quantity we call *visibility* defined in a similar fashion to the quantity in interference optics:

$$v = (|H_z^{(\max)}| - |H_z^{(\min)}|) / (|H_z^{(\max)}| + |H_z^{(\min)}|). \quad (39)$$

Here, $|H_z^{(\min)}|$ and $|H_z^{(\max)}|$ denote the minima and the maxima of modulus of H_z in the region outside a circle of radius $r_{\#}$, if the probe is within the cloaking region, and outside the minimal circle containing the coated cylinder and the probe, if the probe is outside the cloaking region. The values of v are 0.526 for figure 7(a) and 0.021 for figure 7(b), a satisfactorily small value.

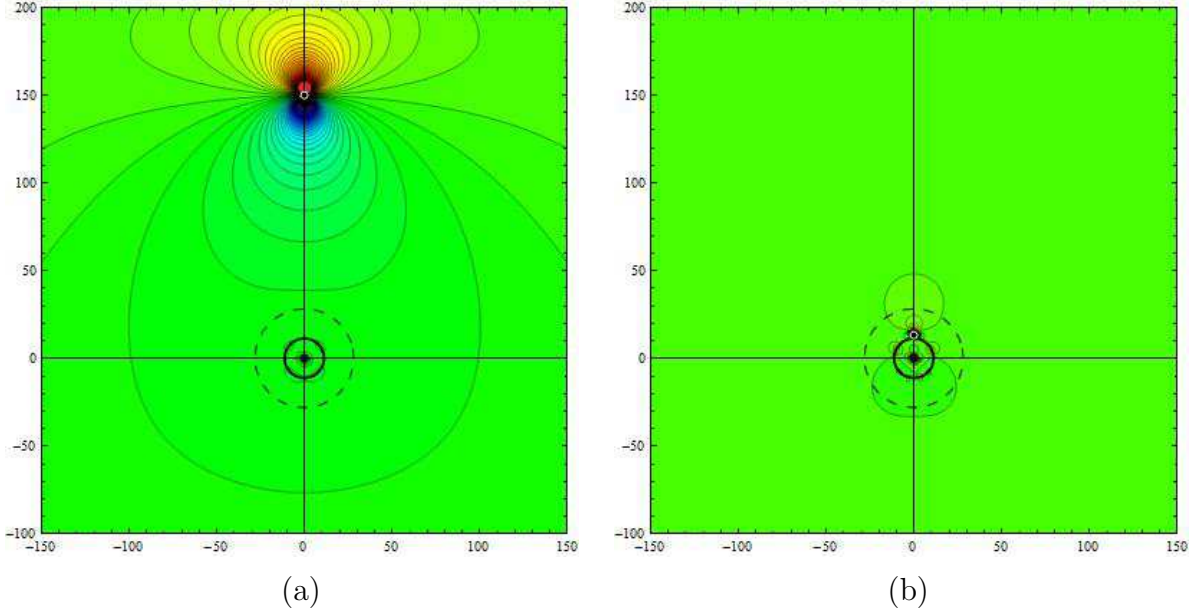


Figure 7. Contour plot of $|H_z|$ as a function of position for a system consisting of a coated cylinder ($r_c = 1.8\text{nm}$, $r_s = 11.25\text{nm}$, $\varepsilon_c = 1$, $\varepsilon_s = -1 + 0.01i$, $\mu_c = \mu_s = 1$) interacting with a probe cylinder ($a = 2\text{nm}$, $\varepsilon = -1 + 0.01i$, $\mu = 1$), and irradiated by a H_z polarized plane wave coming from above. (a): The probe cylinder is outside the cloaking region bounded by the dashed circle, at a distance of 150nm from the origin. (b): The probe cylinder is outside the cloaking region at a distance of 13.5nm from the origin. The visibility (39) takes the values $v = 0.526$ (a) and $v = 0.021$ (b).

5. Conclusions

We have presented numerical results displaying clearly the tendency for it to be more difficult to hide the larger cloaking system than the smaller object it is trying to conceal from electromagnetic probing, and we have analyzed this effect to quantify to what extent it can be overcome. Our results are conveniently summarized in figure 7, and give size limits on the cloaking system in terms of the wavelength. These size limits in fact just require both the cloaking system and the system it is cloaking to be in the quasistatic regime.

We have also shown that this regime in fact sets in at shorter wavelengths for a resonant cloaking system with a small amount of loss, compared with the case of no loss. We have confined our studies to cloaking systems which have spatially uniform shells, but it may be the case that structured systems of the sort described by Farhat *et al* [23] may be designed which inhibit multipole responses in such a way as to ensure the onset of quasistatic behaviour at shorter wavelengths than indicated by figure 7. This would be valuable in possibly simplifying the construction of cloaking systems which operate by plasmonic resonance, while it would be bringing their geometry closer to that of systems which cloak by refraction.

Acknowledgments

Nicolae Nicorovici and Ross McPhedran acknowledge support from the Australian Research Council's Discovery Projects Scheme. The latter's work on this project was also supported by the C.N.R.S., France.

References

- [1] Pendry J B, Schurig D and Smith D R 2006 Controlling electromagnetic fields *Science* **312** 1780–82
- [2] Leonhardt U 2006 Optical conformal mapping *Science* **312** 1777–80
- [3] Nicorovici N A, McPhedran R C and Milton G W 1993 Transport properties of a three-phase composite material: the square array of coated cylinders *Proc. R. Soc. Lond. A* **442** 599–620
- [4] Nicorovici N A, McPhedran R C and Milton G W 1994 Optical and dielectric properties of partially resonant composites *Phys. Rev. B* **49** 8479–82
- [5] Alu A and Engheta N 2005 Achieving transparency with plasmonic metamaterial coatings *Phys. Rev. E* **72** 016623
- [6] Milton G W, Nicorovici N-A P, McPhedran R C and Podolskiy V A 2005 A proof of superlensing in the quasistatic regime, and limitations of superlenses in this regime due to anomalous localized resonance *Proc. R. Soc. Lond. A* **461** 3999–4034
- [7] Milton G W and Nicorovici N-A P 2006 On the cloaking effects associated with anomalous localized resonance *Proc. Roy. Soc. Lond. A* **462** 3027–59
- [8] Nicorovici N A, Milton G W, McPhedran R C and Botten L C 2007 Quasistatic cloaking of two-dimensional polarizable discrete systems by anomalous resonance *Opt. Exp.* **15** 6314–23; Nicorovici N A, Milton G W, McPhedran R C and Botten L C 2007 Supporting online material <http://www.physics.usyd.edu.au/cudos/research/plasmonics/cloakingsystems-appendix-02.pdf>
- [9] Leonhardt U and Philbin T G 2006 General relativity in electrical engineering *New J. Phys.* **8** 247–64

- [10] Kildishev A V and Narimanov E E 2007 Impedance-matched hyperlens *Opt. Lett.* **32** 3432–34
- [11] Schurig D, Mock J J, Justice B J, Cummer S A, Pendry J B, Starr A F and Smith D R 2006 Metamaterial electromagnetic cloak at microwave frequencies *Science* **314** 977–80
- [12] Bruno O P and Lintner S 2007 Superlens-cloaking of small dielectric bodies in the quasistatic regime *J. Appl. Phys.* **102** 124502
- [13] Milton G W, Briane M and Willis J R 2006 On cloaking for elasticity and physical equations with a transformation invariant form *New J. Phys.* **8** 248–67
- [14] Hao-Yuan She, Le-Wei Li, Martin O J F and Mosig J R 2008 Surface polaritons of small coated cylinders illuminated by normal incident TM and TE plane waves *Opt. Exp.* **16** 1007–19
- [15] Min Yan, Zhichao Ruan and Min Qiu 2007 Cylindrical invisibility cloak with simplified material parameters is Inherently Visible *Phys. Rev. Lett.* **99** 233901
- [16] Palik E D (ed) 1991 *Handbook of Optical Constants of Solids* vol I and vol 2 (Boston: Academic Press)
- [17] Felbacq D, Tayeb G and Maystre D 1994 Scattering by a random set of parallel cylinders *J. Opt. Soc. Am. A* **11** 2526–38
- [18] Nicorovici N A, McPhedran R C, Milton G W and Botten L C 2006 Partial Resonances of Three-Phase Composites at Long Wavelengths *Preprint* arXiv:physics/0608247v1 [physics.optics]
- [19] Panofsky W K H and Phillips M 1962 *Classical Electricity and Magnetism* 2nd edn (Reading: Addison-Wesley) p 228
- [20] Abramowitz M and Stegun I A (eds) 1972 *Handbook of Mathematical Functions* (New York: Dover) p 355
- [21] McPhedran R C, Nicorovici N A and Botten L C 1997 The TEM Mode and Homogenisation of Doubly Periodic Structures *J. Electromagn. Waves Appl.* **11** 981
- [22] Van Bladel J G 2007 *Electromagnetic Fields* 2nd edn (New Jersey: Wiley)
- [23] Farhat M, Guenneau S, Movchan A B and Enoch S 2008 Achieving invisibility over a finite range of frequencies *Opt. Exp.* **16** 5656–61